American Mineralogist, Volume 94, pages 1727–1730, 2009

LETTER

Crystal structure of argentopyrite, $AgFe_2S_3$, and its relationship with cubanite

HEXIONG YANG,[1,*] WILLIAM W. PINCH,[2] AND ROBERT T. DOWNS[1]

[1]Department of Geosciences, University of Arizona, Tucson, Arizona 85721-0077, U.S.A.
[2]19 Stonebridge Lane, Pittsford, New York, U.S.A.

ABSTRACT

The structure of argentopyrite, $AgFe_2S_3$, was determined for the first time with single-crystal X-ray diffraction. In contrast to the previously reported orthorhombic symmetry, our data show that argentopyrite is monoclinic with space group $P112_1/n$ (non-standard setting) and unit-cell parameters a = 6.6902(2), b = 11.4497(4), c = 6.4525(2) Å, γ = 90.2420(8)°, and V = 494.26(3) Å^3. Similar to cubanite ($CuFe_2S_3$), the structure of argentopyrite is also based on approximately hexagonal close-packed S atoms, with cations ordered over one half of the tetrahedral sites, forming corner-shared AgS_4 and FeS_4 tetrahedral sheets parallel to (001). The two structures differ chiefly in the linkage between the two adjacent tetrahedral sheets and the ordering patterns of cations within a tetrahedral sheet. Topologically, the structure of argentopyrite can be obtained by a displacement of a tetrahedral sheet in the cubanite structure along the ($\boldsymbol{a}$/2 + $\boldsymbol{b}$/6) direction relative to the sheet beneath, giving rise to a cluster of *four* edge-shared FeS_4 tetrahedra in argentopyrite, as compared to *two* in cubanite. There are *two* distinct Fe sites (Fe1 and Fe2) in argentopyrite, rather than only *one*, as in other MFe_2S_3 sulfide minerals (M = monovalent cations). Together with published Mössbauer data, we suggest that there exists some degree of Fe^{2+}-Fe^{3+} order-disorder in argentopyrite, with Fe^{2+} favoring the more distorted Fe2 tetrahedral site. Argentopyrite appears to possess all the features proposed by Putnis (1977) for a high-temperature ordered form of cubanite.

Keywords: Argentopyrite, $AgFe_2S_3$, Ag-Fe sulfides, cubanite-related mineral, sternbergite, crystal structure, single-crystal X-ray diffraction

INTRODUCTION

Ternary sulfides with a general chemical formula MFe_2S_3, where M represents a monovalent cation, such as Cu^+, Ag^+, K^+, Cs^+, Rb^+, or Tl^+, are characterized by Fe with a nominal valency of +2.5, due to rapid electron exchange between Fe^{2+} and Fe^{3+} ions (Greenwood and Whitfield 1968; Vaughan and Burns 1972; Amthauer and Bente 1983; Wintenberger et al. 1990; McCammon 1994; Reissner et al. 2004; Pareek et al. 2008). These materials exhibit numerous interesting electronic-magnetic properties (Sleight and Gillson 1973; Wintenberger et al. 1990; Reissner et al. 2006), as well as polymorphism at different temperatures or pressures (e.g., Putnis 1977; Miyamoto et al. 1980; McCammon 1994, 1995; Rozenberg et al. 1997; Pruseth et al. 1999). Moreover, different building blocks formed by FeS_4 tetrahedra in the MFe_2S_3 compounds are also found in several enzymes, ferredoxins, and other Fe-S bearing proteins, in which the valence-delocalized [Fe^{2+}-Fe^{3+}] clusters constitute active sites that are responsible for basic electron transfer reactions in many key biochemical pathways (e.g., Holm et al. 1996; Beinert et al. 1997). Geologically, although the MFe_2S_3 minerals, such as cubanite $CuFe_2S_3$, argentopyrite or sternbergite (a dimorph of $AgFe_2S_3$), rasvumite KFe_2S_3, pautovite $CsFe_2S_3$, and picotpaulite $TlFe_2S_3$, are relatively rare when compared to many binary sulfides, they reflect more extreme conditions of ore formation, and thus, may bear important information on geologic occurrence and significance of the various minerals and assemblages involved (Taylor 1970; Osadchii and Chareev 2006).

The crystal structures of all MFe_2S_3 minerals, except argentopyrite, have been previously determined, including cubanite (Buerger 1945, 1947; Azaroff and Buerger 1955; Fleet 1970; Wintenberger et al. 1974; Szymanski 1974; McCammon et al. 1992), sternbergite (Pertlik 1987), rasvumite (Clark and Brown 1980; Mitchell et al. 2004), pautovite (Mitchell et al. 2004), and picotpaulite (Balić-Žunić et al. 2008). A common structural feature of these minerals is that they all contain only one symmetrically nonequivalent tetrahedral Fe site. Their major differences are manifested in the coordination of M cations and the linkage of FeS_4 tetrahedra. In cubanite, each Cu is bonded to four S atoms and each FeS_4 tetrahedron shares one edge with another FeS_4 tetrahedron, forming a cluster of paired FeS_4 tetrahedra. In sternbergite, Ag is also coordinated by four S atoms, but each FeS_4 tetrahedron shares two edges with other FeS_4 tetrahedra, forming a single tetrahedral chain. In the isostructural minerals, rasvumite, pautovite, and picotpaulite, the large M cations are bonded to 10 S atoms and each FeS_4 tetrahedron shares three edges with other FeS_4 tetrahedra to form a double tetrahedral chain.

Argentopyrite and sternbergite are the two best-documented ternary sulfides in the Ag-Fe-S system. Relative to sternbergite, argentopyrite is the stable form at lower temperatures (<150 °C) (Czamanske 1969; Taylor 1970) and is more common in nature. However, despite the long history since its first description (von

* E-mail: hyang@u.arizona.edu

0003-004X/09/1112–1727$05.00/DOI: 10.2138/am.2009.3324

Waltershausen 1866), the presence of severe twining in all examined crystals has prevented the structural determination for this mineral. Argentopyrite from the type locality Joachimstal, Bohemia, Czech Republic, was originally described as monoclinic (von Waltershausen 1866). However, Murdoch and Berry (1954) studied argentopyrite from both Freiberg (Saxony, Germany) and Joachimstal, and concluded that the mineral is orthorhombic with a = 6.64, b = 11.47, c = 6.45 Å, and space group *Pmmn*. They further reported that all minerals examined are markedly pseudohexagonal due to a combination of interpenetrating and lamellar twinning. The chemistry of argentopyrite from Andreasberg (Harz, Germany) was determined by Czamanske (1969) and its Mössbauer spectra by Vaughan and Burns (1972). Šrein et al. (1986) studied mineralogical features of argentopyrite and sternbergite from a polymetallic vein in a skarn deposit (Czech Republic). Since then, no detailed crystallographic study on argentopyrite has been reported. In this paper, we present the first structure solution of argentopyrite based on single-crystal X-ray diffraction data and depict its structural relationships with cubanite and other MFe_2S_3 minerals.

EXPERIMENTAL METHODS

Two argentopyrite samples were used in this study: one from Schaft 209, Aue, Niederschlema, Erzgebirge, Saxony, Germany, and the other from the original type sample (Joachimstal, Bohemia, Czech Republic) (von Waltershausen 1866). Both samples are in the collection of the RRUFF project (deposition no. R090026 and R090027, respectively; http://rruff.info/). Argentopyrite crystals from the two samples appear as simple pseudohexagonal prisms and are bright dark-gray when a fresh surface is exposed, with metallic luster. Their chemical compositions were determined with a JEOL JXA-8900/R electron microprobe at the Geophysical Laboratory of the Carnegie Institution of Washington. The average composition, normalized to S = 3.0, yielded a formula of $Ag_{0.96}Fe_{2.01}S_3$ (9 analysis points) for R090026 and $Ag_{0.97}Fe_{1.99}S_3$ (10 analysis points) for R090027.

A Bruker X8 APEX2 CCD X-ray diffractometer equipped with graphite-monochromatized Mo$K\alpha$ radiation was used for the X-ray diffraction study. Detailed procedures for data collections and processes were similar to those described by Yang and Downs (2008). X-ray diffraction data collected to $2\theta \leq 70°$ show that argentopyrite crystals from the two specimens have similar unit-cell parameters, matching those given by Murdoch and Berry (1954), and both are twinned, with the R090026 sample characterized dominantly by lamellar twinning and R090027 by both pseudohexagonal and lamellar twins. Examination of the X-ray intensity data from both specimens reveals that argentopyrite is actually monoclinic with space group $P112_1/n$, rather than orthorhombic with space group *Pmmn* (Murdoch and Berry 1954). The adaptation of the non-standard setting provides consistency with the published unit-cell data and facilitates direct comparison with other MFe_2S_3 minerals. The structure was solved and refined using SHELX97 (Sheldrick 2008), which yielded the R_1 factors of 0.045 and 0.072 for the R090026 and R090027 samples, respectively.

However, with additional examinations of the argentopyrite crystals from R090026, we successfully found an untwined single crystal with a size of 0.06 × 0.06 × 0.07 mm. A set of X-ray diffraction data were then collected from this crystal. All reflections were indexed on the basis of a monoclinic unit cell (Table 1). The systematic absences of reflections confirm the unique space group $P112_1/n$ and the derived structure solution is identical to that obtained from the data collected from the twinned crystals. A structure refinement with anisotropic displacement parameters for all atoms produced an R_1 factor of 0.029. No significant twin components were detected during the refinement. Final coordinates and displacement parameters of all atoms are listed in Table 2, and selected bond distances and angles in Table 3. CIF[1] on deposit.

TABLE 1. Summary of crystal data and refinement results for argentopyrite

Structural formula	$AgFe_2S_3$
Space group	$P112_1/n$ (no. 14)*
a (Å)	6.6902(2)
b (Å)	11.4497(4)
c (Å)	6.4525(2)
γ (°)	90.2420(8)
V (Å³)	494.26(3)
Z	4
ρ_{calc} (g/cm³)	4.243
λ (Å)	0.71069
μ (mm⁻¹)	10.79
θ range for data collection	3.52–34.95
No. of reflections collected	8409
No. of independent reflections	2144
No. of reflections with $I > 2\sigma(I)$	1652
No. of parameters refined	56
R(int)	0.031
Final R factors [$I > 2\sigma(I)$]	R_1 = 0.029, wR_2 = 0.060
Final R factors (all data)	R_1 = 0.042, wR_2 = 0.064
Goodness-of-fit	1.061

* A non-standard setting (see the text for explanation).

RESULTS AND DISCUSSION

The structure of argentopyrite contains six symmetrically distinct atomic sites: one occupied by Ag, two by Fe (Fe1 and Fe2), and three by S (S1, S2, and S3) (Table 2), and it is analogous to that of cubanite in many aspects. For example, both structures are based on approximately hexagonal close-packed S atoms, with cations ordered over one half of the tetrahedral sites. Topologically, the two structures are composed of the same type of corner-shared tetrahedral sheets parallel to (001) (Fig. 1). One of the key differences between the two structures

[1] Deposit item AM-09-055, CIF. Deposit items are available two ways: For a paper copy contact the Business Office of the Mineralogical Society of America (see inside front cover of recent issue) for price information. For an electronic copy visit the MSA web site at http://www.minsocam.org, go to the American Mineralogist Contents, find the table of contents for the specific volume/issue wanted, and then click on the deposit link there.

TABLE 3. Selected interatomic distances (Å) in argentopyrite

	Distance		Distance		Distance
Ag-S1	2.4985(8)	Fe1-S1	2.2333(8)	Fe2-S1	2.2311(8)
Ag-S1	2.5348(8)	Fe1-S2	2.3095(8)	Fe2-S2	2.2615(7)
Ag-S2	2.5427(7)	Fe1-S3	2.2577(7)	Fe2-S2	2.3136(8)
Ag-S3	2.5557(7)	Fe1-S3	2.3008(8)	Fe2-S3	2.2894(8)
Average	2.5329		2.2753		2.2739
TAV	2.77		7.39		10.62
TQE	1.0006		1.0019		1.0026

Note: TAV = tetahedral angle variance in degrees squared; TQE = tetrahedral quadratic elongation (Robinson et al. 1971).

TABLE 2. Coordinates and displacement parameters of atoms in argentopyrite

Atom	x	y	z	U_{11}	U_{22}	U_{33}	U_{23}	U_{13}	U_{12}	U_{eq}
Ag	0.33197(4)	0.16461(2)	0.38491(4)	0.0313(1)	0.0351(2)	0.0345(2)	–0.0040(1)	0.0003(1)	–0.0034(1)	0.0336(1)
Fe1	0.83066(5)	0.32887(3)	0.37493(6)	0.0146(2)	0.0142(2)	0.0186(2)	–0.0019(1)	0.0004(1)	–0.0008(1)	0.0158(1)
Fe2	0.32872(5)	0.49989(3)	0.37518(6)	0.0131(2)	0.0148(2)	0.0184(2)	–0.0005(1)	–0.0010(1)	–0.0006(1)	0.0154(1)
S1	0.14775(10)	0.34665(6)	0.27103(12)	0.0154(3)	0.0198(3)	0.0261(3)	–0.0041(3)	0.0018(3)	–0.0045(2)	0.0204(2)
S2	0.64979(9)	0.48920(6)	0.26747(11)	0.0147(3)	0.0190(3)	0.0184(3)	0.0023(2)	0.0015(2)	0.0015(2)	0.0174(2)
S3	0.68393(10)	0.17049(5)	0.23119(11)	0.0180(3)	0.0156(3)	0.0186(3)	–0.0039(2)	0.0009(2)	–0.0014(2)	0.0174(2)

Note: U_{ij} are in units of Å².

is the linkage (or relative position) between the two adjacent tetrahedral sheets. Without regard to the chemical contents in the tetrahedra, the structure of argentopyrite can be generated by a displacement of a tetrahedral sheet in the cubanite structure along the (***a***/2 + ***b***/6) direction relative to the tetrahedral sheet beneath. Another noticeable dissimilarity between the two structures is the ordering patterns of M and Fe cations within a tetrahedral sheet. As illustrated in Figure 1, the MS_4 tetrahedron in cubanite is situated at the apical position of a three-member ring, whereas that in argentopyrite is at one of the basal positions. As a consequence, there is a cluster of four edge-shared FeS_4 tetrahedra in argentopyrite, but only two in cubanite (Fig. 2). For comparison, the edge-shared linkage of FeS_4 tetrahedra in sternbergite and rasvumite are also illustrated in Figure 2.

In argentopyrite there are *two* nonequivalent Fe sites, rather than only one, as in other MFe_2S_3 minerals. Although the average Fe-S bond distances for the two FeS_4 tetrahedra are similar, the $Fe2S_4$ tetrahedron appears to be slightly more distorted than the $Fe1S_4$ tetrahedron in terms of the tetrahedral angle variance (TAV) and quadratic elongation (TQE) (Robinson et al. 1971) (Table 3). Intriguingly, Vaughan and Burns (1972) measured Mössbauer spectra of several sulfides containing four-coordinated Fe atoms, including cubanite, sternbergite, and argentopyrite. They noted that, while the Mössbauer spectra of both cubanite and sternbergite consist of only one single hyperfine set of six-lines, as have also been observed by others (Greenwood and Whitfield 1968; Wintenberger et al. 1974, 1990; McCammon 1994, 1995; Rozenberg et al. 1997; Pareek et al. 2008), the spectrum of argentopyrite is clearly characterized by two overlapping six-line sub-spectra, *A* and *B*, of equal intensity, suggesting that Fe in argentopyrite may occur in two distinct tetrahedral positions. This observation is evidently supported by our structural data. The room-temperature isomer-shift and quadrupole-splitting parameters are 0.49 and 2.36 (mm/s), respectively, for subspectrum *A* and 0.35 and 2.21 (mm/s) for subspectrum *B*. These values indicate that subspectrum *A* is of more ferrous character than subspectrum *B* (Vaughan and Burns 1972) and corresponds to a more distorted FeS_4 tetrahedron. Accordingly, we attribute subspectra *A* and *B* to originating from the $Fe2S_4$ and $Fe1S_4$ tetrahedra, respectively. In other words, unlike other MFe_2S_3 minerals (e.g., cubanite, sternbergite, and rasvumite) that show complete disorder between Fe^{2+} and Fe^{3+}, argentopyrite exhibits some degree of cation ordering, with Fe^{2+} favoring the slightly more distorted Fe2 tetrahedral site.

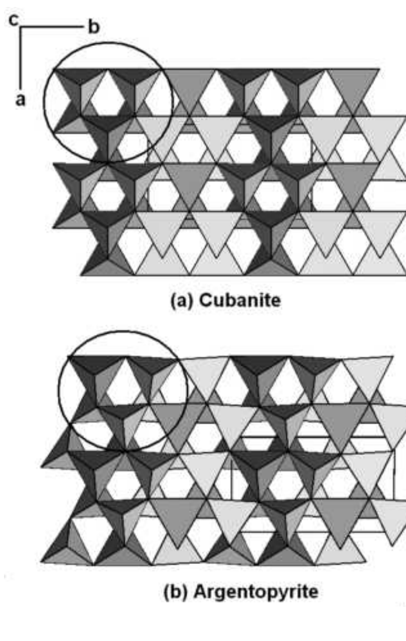

FIGURE 1. Comparison of crystal structures of (**a**) cubanite and (**b**) argentopyrite. The green and yellow tetrahedra represents MS_4 and FeS_4 groups (M = Cu for cubanite and Ag for argentopyrite), respectively. A three-member ring of tetrahedra in each structure is outlined with a circle, showing the positional difference of the MS_4 tetrahedra.

From the crystal-chemical point of view, the preference of Fe^{2+} for the Fe2 site over the Fe1 site may be explained by how the $Fe1S_4$ and $Fe2S_4$ tetrahedra are linked to each other within a cluster. As shown in Figure 2, each $Fe2S_4$ tetrahedron shares two edges with adjacent tetrahedra: one with the $Fe1S_4$ tetrahedron and the other with another $Fe2S_4$ tetrahedron. In contrast, each $Fe1S_4$ tetrahedron shares only one edge with a neighboring $Fe2S_4$ tetrahedron. As a result, not only is the $Fe2S_4$ tetrahedron more distorted than the $Fe1S_4$ tetrahedron, but it is also more energetically favored by Fe^{2+} so as to minimize the cation-cation repulsion between the two edge-shared $Fe2S_4$ tetrahedra and within the cluster. Additionally, the Jahn-Teller effect may play a role in enhancing the order of Fe^{2+} in the Fe2 site as well because high-spin Fe^{2+} can gain extra stabilization energy in a more distorted tetrahedral environment (Vrajmasu et al. 2004 and references therein). The relatively longer distance between Fe2-Fe2 [2.8013(7) Å] vs. Fe2-Fe1 (2.7502 Å) is also a good indication of the enrichment of Fe^{2+} in the Fe2 site (see review by Makovicky 2006).

Cubanite is known to transform irreversibly to a disordered cubic polymorph, isocubanite, at ~210 °C (Pruseth et al. 1999 and references therein). Annealing of the cubic phase below 210 °C results in exsolution of chalcopyrite from the isocubanite matrix (Cabri et al. 1973; Dutrizac 1976). However, using in-situ high-temperature transmission electron microscopy, Putnis (1977) found that cubanite actually starts to undergo the cation disordering process at ~200 °C, giving rise to a hexagonal wurtzite-type structure. Annealing of the hexagonal phase below 200 °C yields a high-temperature ordered (HTO) phase that Putnis (1977) claimed was probably orthorhombic. Although the unit-cell parameters of this HTO phase are similar to those of cubanite, we find that its symmetry is definitely different from that (*Pcmn*) for cubanite because the electron diffraction patterns given by Putnis (1977) show the presence of (*h*00) and (00*l*) reflections with *h* or $l \neq 2n$, which are prohibited in space group *Pcmn*. By assuming that the transformation from the disordered hexagonal to the HTO phase results from cation ordering within the hexagonal close-packed sulfur structure, Putnis (1977) proposed a

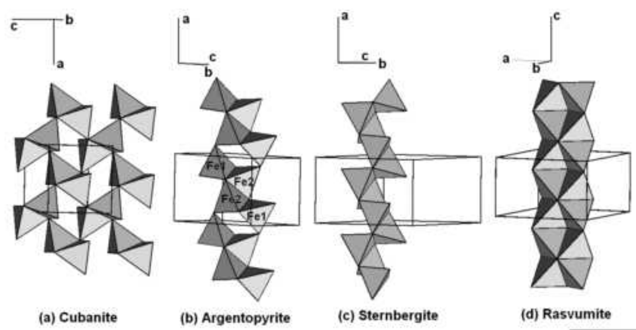

FIGURE 2. Comparison of the linkage among the FeS_4 tetrahedra in (**a**) cubanite, (**b**) argentopyrite, (**c**) sternbergite, and (**d**) rasvumite.

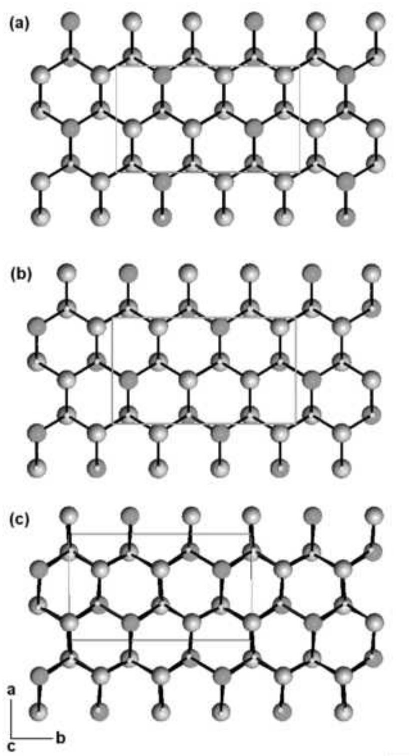

FIGURE 3. Cation ordering schemes in (**a**) cubanite, (**b**) high-temperature ordered phase of cubanite, proposed by Putnis (1977), and (**c**) argentopyrite. They are represented in terms of sulfur atoms coordinated by metal cations. Green, gray, and small yellow spheres represent M (=Cu in cubanite or Ag in argentopyrite), Fe, and S atoms, respectively.

possible cation ordering scheme for the HTO phase that is better viewed in terms of the distribution of sulfur atoms coordinated by metal cations (Fig. 3). Analysis of the atomic distribution in Figure 3b, nevertheless, reveals that such a structure can only have symmetry lower than orthorhombic, though it may display a pseudo-orthorhombic unit cell. In fact, irrespective of the chemical difference in the M cation, the atomic arrangement in Figure 3b is just what we have observed in argentopyrite—a pseudo-orthorhombic cell with $P112_1/n$ symmetry (Fig. 3c). Additional research is needed to verify whether the HTO phase of cubanite really possesses the argentopyrite-type structure. If that is the case, then argentopyrite might transform to the cubanite structure upon application of pressure.

ACKNOWLEDGMENTS

This study was supported by the NSF grant EAR-0609906 for the study of bonded interactions of sulfide minerals. The samples used in this study were kindly donated by Mark N. Feinglos. We are grateful for the electron microprobe analysis by N. Boctor at the Geophysical Laboratory. The constructive reviews from Emil Makovicky and Milan Rieder are greatly appreciated.

REFERENCES CITED

Amthauer, G. and Bente, K. (1983) Mixed-valent iron in synthetic rasvumite, KFe_2S_3. Naturwissenschaften, 70, 146–147.
Azaroff, L.V. and Buerger, M.J. (1955) Refinement of the structure of cubanite, $CuFe_2S_3$. American Mineralogist, 40, 213–225.
Balić-Žunić, T., Karanović, L., and Poleti, D. (2008) Crystal structure of picotpaulite, $TlFe_2S_3$, from Allchar, FYR Macedonia. Acta Chimica Slovenica, 55, 801–809.
Beinert, H., Holm, R.H., and Munck, E. (1997) Iron-sulfur clusters: Nature's modular, multipurpose structures. Science, 277, 653–659.
Buerger, M.J. (1945) The crystal structure of cubanite, $CuFe_2S_3$ and the coordination of ferromagnetic iron. Journal of the American Chemical Society, 67, 2056.
——— (1947) The crystal structure of cubanite. American Mineralogist, 32, 415–425.
Cabri, L.J., Hall, S.R., Szymanski, J.T., and Stewart, J.M. (1973) On the transformation of cubanite. Canadian Mineralogist, 12, 33–38.
Clark, J.R. and Brown Jr., G.E. (1980) Crystal structure of rasvumite, KFe_2S_3. American Mineralogist, 65, 477–482.
Czamanske, G.K. (1969) The stability of argentopyrite and sternbergite. Economic Geology, 64, 459–461.
Dutrizac, J.E. (1976) Reactions in cubanite and chalcopyrite. Canadian Mineralogist, 14, 172–181.
Fleet, M.E. (1970) Refinement of the crystal structure of cubanite and polymorphism of $CuFe_2S_3$. Zeitscrift für Kristallographie, 132, 276–287.
Greenwood, N.N. and Whitfield, H.J. (1968) Mössbauer effect studies on cubanite and related iron sulfides. Journal of the Chemical Society (London) A, 1697–1699.
Holm, R.H., Kennepohl, P., and Solomon, E.I. (1996) Structural and functional aspects of metal sites in biology. Chemical Reviews, 96, 2239–2314.
Makovicky, E. (2006) Crystal structures of sulfides and other chalcogenides. In D.J. Vaughan, Ed., Sulfide Mineralogy and Geochemistry, 61, p. 7–125. Reviews in Mineralogy and Geochemistry, Mineralogical Society of America, Chantilly, Virginia.
McCammon, C.A. (1994) High-pressure in situ investigation of cubanite ($CuFe_2S_3$): Electronic structure. Hyperfine Interactions, 93, 1511–1514.
——— (1995) Equation of state, bonding character and phase transition of cubanite, $CuFe_2S_3$ studied from 0 to 5 GPa. American Mineralogist, 80, 1–8.
McCammon, C.A., Zhang, J., Hazen, R.M., and Finger, L.W. (1992) High-pressure crystal chemistry of cubanite $CuFe_2S_3$. American Mineralogist, 77, 937–944.
Mitchell, R.H., Ross, K.C., and Potter, E.G. (2004) Crystal structures of $CsFe_2S_3$ and $RbFe_2S_3$: synthetic analogs of rasvumite KFe_2S_3. Journal of Solid State Chemistry, 177, 1867–1872.
Miyamoto, M., Ishii, T., Kume, S., and Koizumi, M. (1980) A new polymorph of cubanite, $CuFe_2S_3$. Materials Research Bulletin, 15, 907–910.
Murdoch, J. and Berry, L.G. (1954) X-ray measurements on argentopyrite. American Mineralogist, 39, 475–485.
Osadchii, E.G. and Chareev, D.A. (2006) Thermodynamic studies of pyrrhotite-pyrite equilibria in the Ag-Fe-S system by solid-state galvanic cell technique at 518–723 K and total pressure of 1 atm. Geochimica et Cosmochimica Acta, 70, 5617–5633.
Pareek, S., Rais, A., Tripathi, A., and Chandra, U. (2008) Mössbauer study on microwave synthesized (Cu,Fe) sulfide composites and correlation with natural mineral—Cubanite. Hyperfine Interactions, 186, 113–120.
Pertlik, F. (1987) Crystal structure of sternbergite, $AgFe_2S_3$. Neues Jahrbuch für Mineralogie, Monatshefte, 10, 458–464.
Pruseth, K.L., Mishra, B., and Bernhardt, H.J. (1999) An experimental study on cubanite irreversibility: Implications for natural chalcopyrite-cubanite intergrowths. European Journal of Mineralogy, 11, 471–476.
Putnis, A. (1977) Electron microscope study of phase transformation in cubanite. Physics and Chemistry of Minerals, 1, 335–349.
Reissner, M., Steiner, W., and Holler, H. (2004) ^{57}Fe Mössbauer investigation of $K_{0.3}Ba_{0.7}Fe_2S_3$. Journal of Alloys and Compounds, 383, 131–134.
Reissner, M., Steiner, W., Wernisch, J., and Boller, H. (2006) Debye temperature and magnetic ordering in $K_xBa_{1-x}Fe_2S_3$. Hyperfine Interactions, 169, 1301–1304.
Robinson, K., Gibbs, G.V., and Ribbe, P.H. (1971) Quadratic elongation, a quantitative measure of distortion in coordination polyhedra. Science, 172, 567–570.
Rozenberg, G.Kh., Pasternak, M.P., Hearne, G.R., and McCammon, C.A. (1997) High-pressure metallization and electronic-magnetic properties of hexagonal cubanite ($CuFe_2S_3$). Physics and Chemistry of Minerals, 24, 569–573.
Sheldrick, G.M. (2008) A short history of SHELX. Acta Crystallographica, A64, 112–122.
Sleight, A.W. and Gillson, J.L. (1973) Electrical resistivity of cubanite: $CuFe_2S_3$. Journal of Solid State Chemistry, 8, 29–30.
Šrein, V., Řídkošil, T., Kašpar, P., and Šourek, J. (1986) Argentopyrite and sternbergite from polymetallic veins of the skarn deposit Měděnec, Krušné hory Mts., Czechoslovakia. Neues Jahrbuch für Mineralogie, Abhandlungen, 154, 207–222.
Szymanski, J.T. (l974) A refinement of the structure of cubanite, $CuFe_2S_3$. Zeitschrift für Kristallogaphie, 140, 218–239.
Taylor, L.A. (1970) The system Ag-Fe-S: Phase equilibria and mineral assemblages. Mineralogical Deposita, 5, 41–58.
Vaughan, D.J. and Burns, R.G. (1972) Mössbauer spectroscopy and bonding in sulphide minerals containing four-coordinated iron. Report of the Session International Geological Congress 24th, 14, 158–167.
von Waltershausen, W.S. (1866) Der silberkies, eine neue mineralspecies aus Joachimsthal. Gottingische Gelehrte Anzeigen, 3, 2–8.
Vrajmasu, V.V., Munck, E., and Bominaar, E.L. (2004) Theoretical analysis of the Jahn-Teller distortions in tetrathiolato iron(II) complexes. Inorganic Chemistry, 43, 4862–4866.
Wintenberger, M., Lambert-Andron, B., and Roudaut, E. (1974) Détermination de la structure magnétique de la cubanite par diffraction neutronique sur un monocristal. Physica Status Solidi, A26, 147–154.
Wintenberger, M., Andre, G., Perrin, M., Garcin, C., and Imbert, P. (1990) Magnetic structure and Mössbauer data of sternbergite $AgFe_2S_3$, an intermediate valency Fe compound. Journal of Magnetism and Magnetic Materials, 87, 123–129.
Yang, H. and Downs, R.T. (2008) Crystal structure of glaucodot, (Co,Fe)AsS, and its relationships to marcasite and arsenopyrite. American Mineralogist, 93, 1183–1186.

MANUSCRIPT RECEIVED JUNE 18, 2009
MANUSCRIPT ACCEPTED JULY 22, 2009
MANUSCRIPT HANDLED BY BRYAN CHAKOUMAKOS